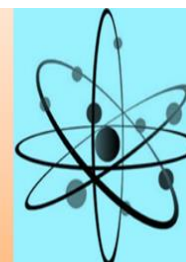




## Journal of Physical Chemistry and Functional Materials (JPCFM)

journal homepage: <http://dergipark.gov.tr/jphcfum>



Received: 14 July 2018

Accepted: 31 July 2018

Research Article

### Geostatistical Modelling for $^{134}\text{Cs}$ Released from The Fukushima Radioactive Fallout

Sevim Bilici<sup>1,2\*</sup>, Ahmet Bilici<sup>1,2</sup>, Fatih Kulahci<sup>1</sup>

<sup>1</sup>Nuclear Physics Division, Physics Department, Firat University, Elazig, Turkey.

<sup>2</sup>Department of Opticianry, Vocational School of Health Service, Bartin University, Bartin, Turkey.

\*Corresponding Author: [sbilici@bartin.edu.tr](mailto:sbilici@bartin.edu.tr)

#### Abstract

The distribution of radionuclides show variability as spatially. For this reason, determining the spatial distribution is very important. In the study, spatial analysis technique using as Point Cumulative Semivariogram (PCSV) method is modelled for the radioactive fallout which had occurred after the Fukushima Dai-Ichi Nuclear Power Plant accident. The theoretical basis of the Point Cumulative Semivariogram (PCSV) method is based to variogram analysis. PCSV allow the regionalized behavior of variables into use. PCSV modelling is applied for  $^{134}\text{Cs}$  radionuclide in soil samples in the accident area. 5 different models are obtained to determine the transport properties and distribution of  $^{134}\text{Cs}$ .

**Key Words:** Fukushima; Radioactive Fallout; Spatial Analysis; Point Cumulative Semivariogram;  $^{134}\text{Cs}$  Transport; Modelling.

## 1. Introduction

The Fukushima Daiichi Nuclear Power Plant (FDNPP) was severely damaged on March 11, 2011 after the big earthquakes. After the accident, extremely amounts of radionuclides were released in atmosphere and ocean [1]. The radioactive cesium obtained from the FDNPP accident spread over a large area in the northeastern half of Honshu, the main island of Japan. [2,3]. Many researchers in the literature have studied the distribution and transport of radioactive cesium and have presented various important findings [3-8].

In this study, after the FDNPP accident, the Point Totals Semivariogram method, one of the spatial analysis methods, was used to have practical knowledge about the distribution of radioactive  $^{134}\text{Cs}$  in the soil. This method is based on the regional variable theory in geostatistics. Regional variables have continuity between points. Relation of the regional variables to the distance is done with the variogram (or Semi-variogram). Semivariogram characterizes and interprets the spatial relationships of natural phenomena.

## 2. Material and Methods

### Research Area

In this study, after the Fukushima reactor accident, a spatial analysis model was made for the radioactive fallout from the stream. The methodology was applied for  $^{134}\text{Cs}$  radioisotope in soil samples in the accident site. We used radionuclide data reported by Japanese Government. 81 different sampling points used in the study area and model are given in Figure 1.

Graphs showing the spatial distribution and transport of the  $^{134}\text{Cs}$  artificial radionuclide in these stations were drawn and interpreted. As a result, 5 different models were obtained. The stations representing these models were shown in different colors on the map.

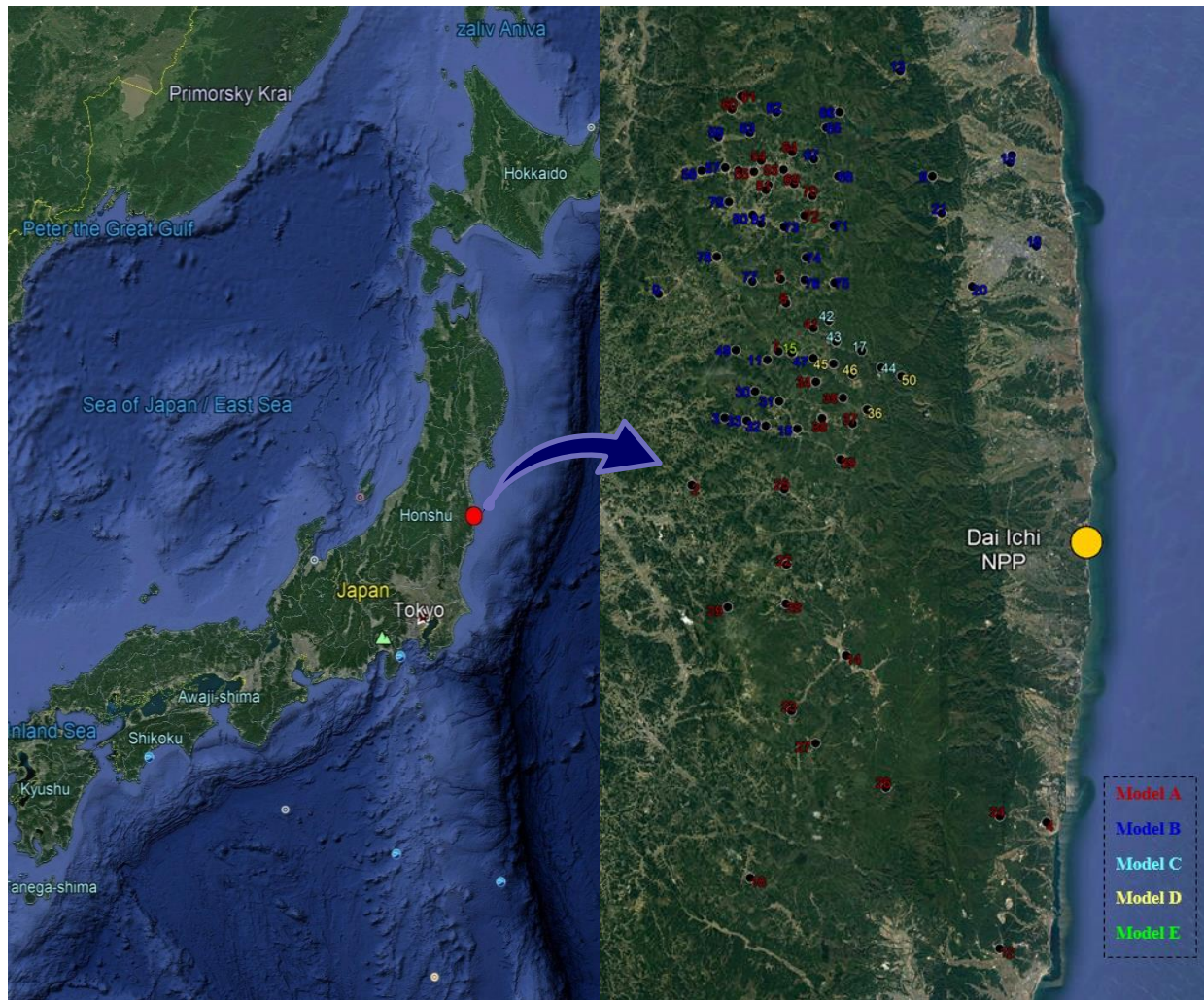


**Figure 1.** Research area and sampling stations

### Point Cumulative Semivariogram

Geostatistics explains the distance dependent changes of regional variables in the light of statistical concepts. Basis of Geostatistical is based on the idea that the same variable that is close to each other has a great similarity and as distance goes away this similarity diminishes and eventually ends as distance goes away. This situation is described as the fact that events have spatial correlation [9]. The difference between the values of the regional variables in different positions is

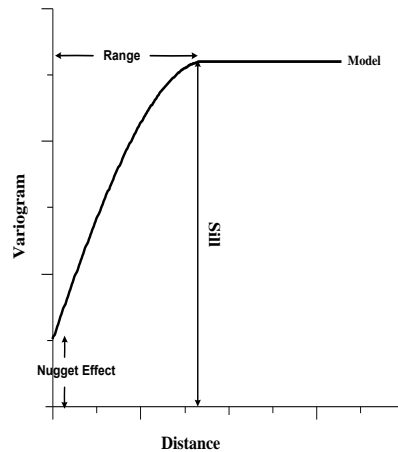
a function of the distance between these variables. [10]. The grade of the spatial continuity of the regional variable is expressed by the Semivariogram (YV) function.

YV is expressed as the variance of the difference between regional variables and the general equation (1) is as follows. The semivariogram is used to determine what characteristics the relevant variable represents [11].

$$\gamma_h = \frac{1}{2N_d} \sum_{i=1}^{N_d} (X_i - X_{i+d})^2 \quad (1)$$

Here  $\gamma_h$  is the YV value at distance  $h$ ;  $X_i$  is the value of the regional variable in position  $i$ ;  $X_{i+d}$  is the value of the regional variable measured after the distance  $d$  from  $i$ ;  $N_d$  is the total number of sample distances. If  $h$  represents small distances, the compared points will start at values close to each other, and thus the YV values will be small. If this distance is increased, the compared points will be less related to each other, the differences will start to increase and therefore large YV values will be obtained.

YV model is generally defined by three parameters: range of influence, Nugget effect, and Sill. The representation of these parameters on a YV model is given in Figure 2.

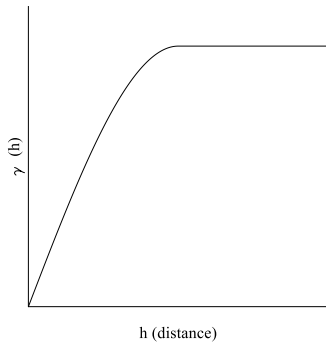
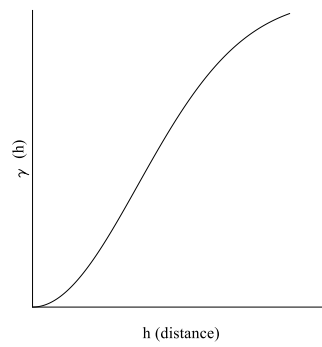
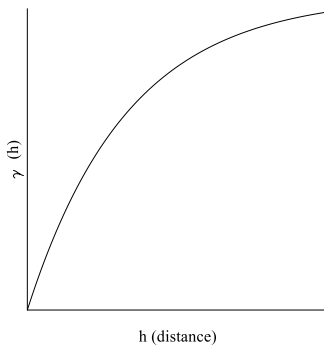
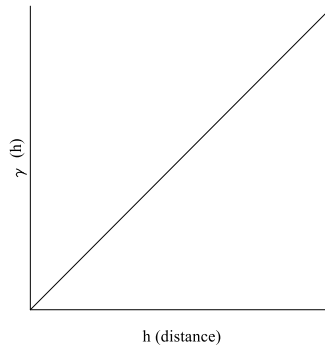


**Figure 2.** Semivariogram Parameters

The distance-of-influence range is the distance value that remains within a region and is a distance from a specified point to another point that affects the value of that point. Points outside this distance have no effects to value at the specified point. Sill is the point where the YV function is fixed. The near original behavior of YV gives information about the continuity of the regional variability. Parabolic shape a changing feature, while linear shape shows the continuous increase or decrease of the regional variable the discontinuity in the origin determines measurement errors or small scale changes [12-17]. The distance between two sample points closest to each other is the smallest distance at which the change can be determined. At smaller distances from this distance, the change in the difference between the values can not be determined. This causes the YV to assume a positive value other than zero at the origin. This situation is known as the NV effect in YV.

It is necessary to know the YV at all distances in determining the properties of the regional variable, and in particular in estimating the values at the unsampled points. This requires modeling YV, that is, adapting a function to YV values. Since YV always takes positive values, it must be a positive defined function in the function to be selected. There are many YV models. Some of them are: spherical model, gauss model, exponential model and Linear model.

When the nugget effect is found in the model, raw model is shifted up the unit by adding the number  $C_0$ . Thus, nugget is obtained effective model.

**Figure 3.** Spherical Model**Figure 4.** Gauss model**Figure 5.** Exponential Model**Figure 6.** Linear model

Semi-Variogram can be applied when the regional variable is stable and in situation regularly distributed. As the distance increases, the number of data pairs decreases for the calculation of YV. This means less reliable forecasting at large distances. Hence, YV gives reliable results for close distances between the sample points in the study area, but the reliability of the YV decreases as the distance increases [18].

The YV calculation process is similar to the time series analysis. YV is the degree of distance and area dependency between uniformly scattered points. At the beginning of the acceptance of YV, there is area relation depending on stationarity and equal distances. Rather than a point relationship is a matter of properly distributed field relations [19]. In the absence of stability, the relation between randomly distributed points can not be examined with the YV approach. [14]. In order to avoid these deficiencies, Point Total Semi-Variogram (NTYV) method was developed by Şen (1989), which relies on the relation between point and field according to the absence of stability and the random distribution of points.

The NTYV method state to the regional effect of all other stations within the study area on a particular station. Thus, the number of NTYVs is equal to the number of stations [5,15]. NTYV can be defined as the sum of half of the differences squared that from small to large listed correctly in terms of distance. This method gives a non-decreasing function of the NTYV example at the location. Mathematical expression is given by equation (2) [5].

$$\gamma(d_i) = \frac{1}{2} \sum_{i=1}^{n-1} (Z_c - Z_i)^2 \quad (2)$$

Where  $\gamma(d_i)$  is the NTYV value at the  $d_i$  locus of the corresponding station,  $Z_c$  is the regional variable value at the reference point,  $Z_i$  ( $i = 1, 2, \dots, n-1$ ) represents the value of the regional variable at the other surrounding stations. The total number of stations is  $n$ .

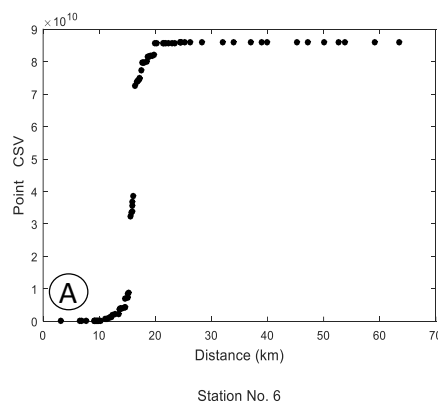
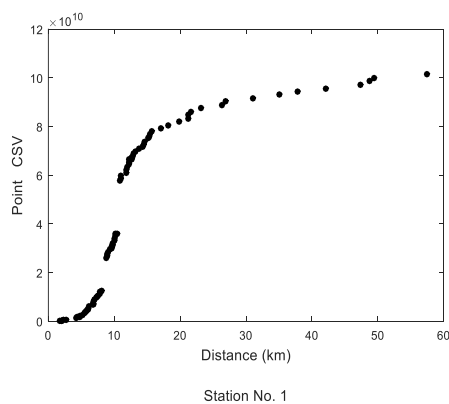
The implementation steps of the NTYV method are as follows:

1. The reference position is selected,  $c$ , the distances between this selected point and the other stations ( $i = 1, 2, \dots, n-1$ ) are calculated. If there are  $n$  positions,  $n-1$  is the difference distance.
2. For each pair, is found half-square differences between the data values. In this way, each distance will have its own semi-square value  $\frac{1}{2}(Z_c - Z_i)^2$ . Where  $Z_c$  and  $Z_i$  are the values of the regional variable in the corresponding region and the  $y$  position, respectively.
3. The distances are sorted from small to large and the sum of consecutive half-square differences against distance is calculated. This method gives a non-decreasing function of the NTYV example at the location. Mathematical expression is given by equation (2).
4. For NTYV given  $n$  sample, the previous steps are applied taking into account the different relevant areas.
5. The NTYV values corresponding to the distance values of each point are marked on the  $y$ -axis so that the NTYV scattering diagram is obtained.

As a result of the existence of a curve representing this scatter diagram, the theoretical NTYV model, namely the function of changing the regional variable by distance is obtained.

### 3. Results and Discussion

The average concentration of  $^{134}\text{Cs}$  is 24699.7 Bq/kg. The position of the study area and the values of  $^{134}\text{Cs}$  are shown in Table 1. The highest concentration of  $^{134}\text{Cs}$  is 26.333.3 Bq/kg at the 44th station with and the lowest density is at station 18 with 641.2 Bq/kg. PCSV charts were obtained up to the number of stations because of total of 81 stations. Figure 7 shows different PCSV plots representing the spatial distribution of  $^{134}\text{Cs}$  in the stations. Since there are PCSV charts that represent the same model, they are broken down into categories as shown in Figure 8 for proper evaluation. The stations of the specified models are given in Table 2.



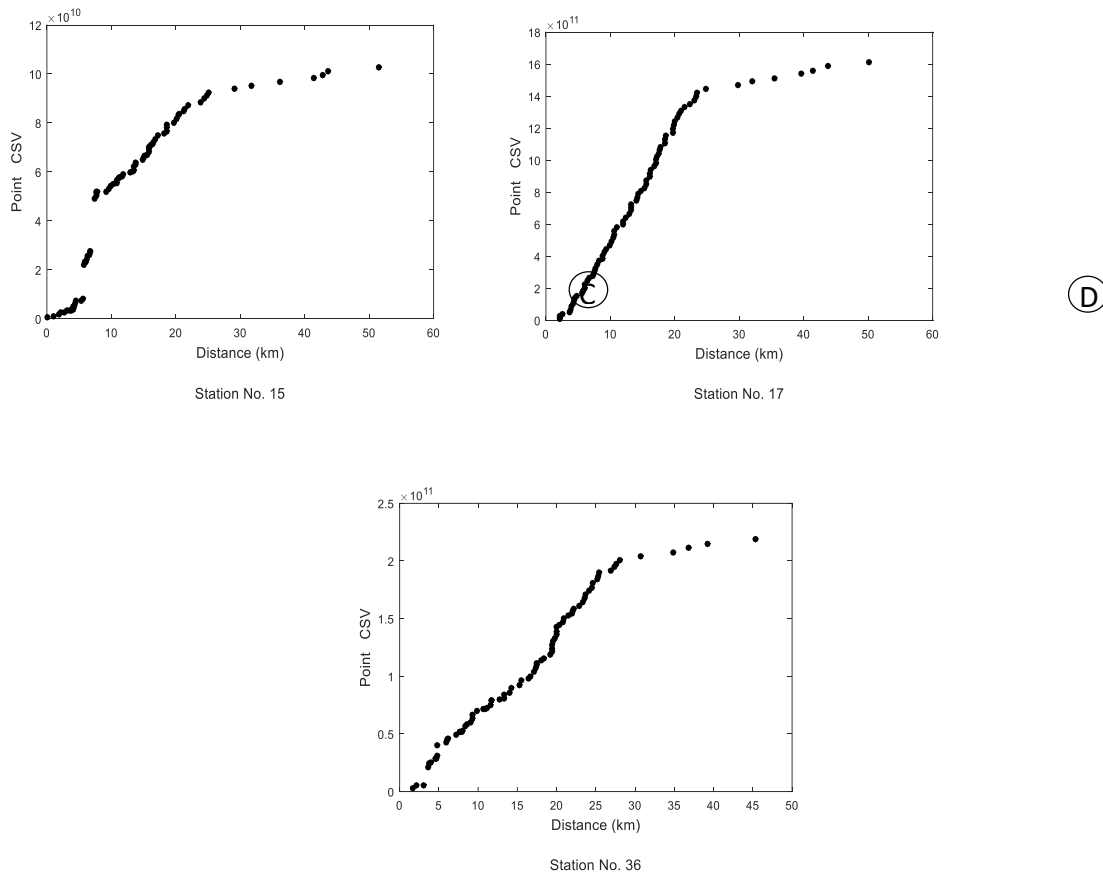
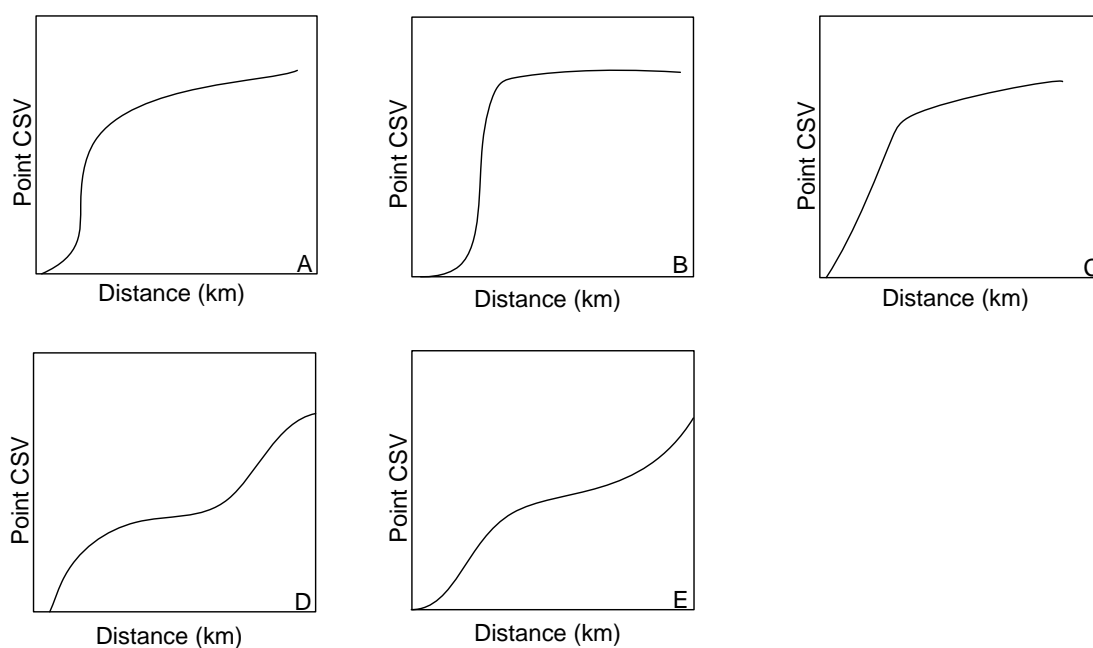


Figure 7. PCSV models for <sup>134</sup>Cs

Table 1. <sup>134</sup>Cs radioactivity levels and their locations

Station no.	Latitude	Longitude	<sup>134</sup> Cs (Bq/kg)	Station no.	Latitude	Longitude	<sup>134</sup> Cs (Bq/kg)
1	37,612803	140,749111	54826,39	42	37,582750	140,793611	74500,00
2	37,462186	140,667572	2219,06	43	37,567417	140,800389	50368,33
3	37,511156	140,697913	8187,04	44	37,548333	140,842056	263333,33
4	37,214403	140,994672	1723,91	45	37,551000	140,797778	73500,00
5	37,706044	140,964325	3168,97	46	37,542944	140,815361	68333,33
6	37,690103	140,889811	1768,96	47	37,555139	140,779194	14016,67
7	37,560025	140,747136	26090,91	48	37,559278	140,759694	20740,00
8	37,595000	140,754017	60748,68	49	37,560389	140,708083	3409,09
9	37,601444	140,636667	13798,04	50	37,542083	140,860667	46137,78
10	37,700150	140,962647	1788,00	51	37,678222	140,735194	23272,73
11	37,553833	140,736731	18800,00	52	37,681889	140,737444	11200,00
12	37,121783	140,951067	1908,89	53	37,693278	140,751500	13350,00
13	37,767864	140,859961	3266,00	54	37,699778	140,730861	15570,00
14	37,337889	140,809489	2583,73	55	37,691694	140,724056	12930,00
15	37,559156	140,759347	55282,05	56	37,692750	140,709750	26909,09
16	37,638739	140,986842	1258,00	57	37,694667	140,697500	14890,00

				220000,0			
17	37,560550	140,823883	0	58	37,692417	140,675611	10010,00
18	37,175842	140,721517	641,19	59	37,716778	140,691139	15427,27
19	37,503417	140,764472	8734,04	60	37,737639	140,703639	21454,55
20	37,608722	140,926750	7258,91	61	37,747056	140,712278	22109,09
21	37,662889	140,898556	7774,55	62	37,735750	140,744944	12154,55
22	37,404307	140,754797	1332,73	63	37,720083	140,720306	10493,64
23	37,297694	140,759306	1533,64	64	37,706500	140,759556	29527,27
24	37,219487	140,951167	1053,82	65	37,724333	140,790972	7663,64
25	37,459460	140,752560	9829,62	66	37,737000	140,803167	1295,45
26	37,241944	140,845928	2772,73	67	37,700639	140,779750	7209,09
27	37,274420	140,781580	3509,00	68	37,688139	140,802083	11509,09
28	37,375861	140,754280	1400,00	69	37,682778	140,761389	16350,00
29	37,373610	140,701500	3225,45	70	37,674028	140,778194	16700,00
30	37,530417	140,725722	7281,82	71	37,652000	140,798028	8520,00
31	37,523306	140,747889	4663,64	72	37,659528	140,770833	28600,00
32	37,505472	140,735444	4025,00	73	37,651167	140,752000	16534,00
33	37,509278	140,718056	5650,00	74	37,628444	140,772556	34151,00
34	37,537510	140,781720	17866,67	75	37,610250	140,798667	26372,73
35	37,525806	140,806528	15200,00	76	37,612056	140,771222	55454,55
36	37,517306	140,828806	86350,00	77	37,610750	140,722944	27372,73
37	37,507000	140,815417	9883,33	78	37,628750	140,690278	13536,36
38	37,511028	140,787250	6916,67	79	37,669222	140,701000	27909,09
39	37,481167	140,804222	6383,33	80	37,659917	140,722972	25809,09
40	37,597278	140,753056	61183,33	81	37,653444	140,730917	24000,00
41	37,577083	140,779361	46166,67				



**Figure 8.** PCSV models for  $^{134}\text{Cs}$



**Table 2.** The PCSV model categories for  $^{134}\text{Cs}$ 

PCSV Models	Station Number
Model A	1,2,4,7,8,12,14,18,22-29,34,35,37-41,51-56,60,61,64,69,70,72
Model B	3,5,6,9-11,13,16,19,20,21,30-33,47-49,57-59,62,63,65-68,71,73-81
Model C	17,42-44
Model D	36,45,46,50
Model E	15

Model A indicates that the variable is a weak change at short and long distances and a strong change at mid distances. Model A shows exponential increase and means increasing gradually of influence incoming from the environmental to this stations. Namely means that the  $^{134}\text{Cs}$  at these stations also affect the intensities of  $^{134}\text{Cs}$  at other stations. Model A cuts the distance axis. This indicates that the density of  $^{134}\text{Cs}$  at lower distances from the cut-off point is low and almost unchanged.

The radius of influence equals the distance at which the variable is active. The effect radius gives information about the range for the transport of values of  $^{134}\text{Cs}$ . Model B has a radius of effect ranging from 17 to 29 km. This indicates that there is no effect of other stations after 17-29 km. Also, PCSV's fixed point is defined as Sill. The distribution of the B model up to the Sill value resembles the Gaussian curve. Ideally, the distance between the sampling points increases the variogram value and rises to a constant value at a certain separation distance. Being of Sill value can be explained as the contribution from other distant stations is weak. When the  $^{134}\text{Cs}$  PCSV charts are examined, it is seen that the sill value is in the range of  $7,5 \cdot 10^{11}$ - $8,6 \cdot 10^{11}$ . The large Sill value at the same effect point indicates that the model curve approaches the PCSV axis and the PCSV values increase. This explains greater the contribution from the other stations to the distribution of the  $^{134}\text{Cs}$ . The distance up to Sill is the distance of effect, which indicates that the spatial dependence is continuing. The large impact distance (range) indicates that the variable is effective at longer distances. Samples separated by greater distance than the effect distance are not spatially related. When these graphs are examined, it is observed that the range value of each graph differs. This difference, the distance from each station to other stations are due to the differences and from environmental factors.

Model C is a linear model that intersects the x-axis. This means that the variable is homogeneously dispersed around the stations matching to model and that this distribution has a uniform distribution. It does not have a Sill value.

Model D, which shows a parabolic behavior in the origin, indicates that the contribution from the other stations to the relevant station is variable and discontinuous. In the D model, the sill or radius of effect is not observed.

Model E shows a corresponding change to the Gauss model and then goes into a sudden increase. The Gaussian model expresses events that are similar at extremely continuous or short distances. It is possible to make an interpretation that there is a lot of transport in the locations where the 15. station is

located and that the location patterns have a different effect here. The sudden increase in the PCSV graph in the model can be explained in this way. Due to its geological location, the contribution from near environmental the station is much different from the contribution from the distant stations. Therefore, these two opposite states can create suddenly changing conditions on this station.

When the graphics are examined in general; The PCSV graphs of the  $^{134}\text{Cs}$  values observed in the soil samples showed 5 different models. It was observed that the  $^{134}\text{Cs}$  radionuclide concentrations in the identified models showed similar and different distributions. Information about the mobility at stations of  $^{134}\text{Cs}$  was obtained. Different distributions indicate that affected in different formats from environmental factors in stations. For similar distributions, it is possible to say that the contributions to each other of the stations and the environmental factors are partly equal to the behavior of the radionuclide.

## References

- [1] N. Yoshida, Y. Takahashi, Land-surface contamination by radionuclides from the Fukushima Daiichi Nuclear Power Plant accident. *Elements* 8 (2012) 201–206.
  - [2] K. Hirose, 2011 Fukushima Dai-ichi Nuclear Power Plant accident: summary of regional radioactive deposition monitoring results. *J Environ Radioact* 111 (2012) 13–17.
  - [3] T.J. Yasunari, A. Stohl, R.S. Hayano, J.F. Burkhart, S. Eckhardt, T. Yasunari, Cesium-137 deposition and contamination of Japanese soils due to the Fukushima nuclear accident. *PNAS* 108 (2011) 19530–19534.
  - [4] S. Niksarlıoğlu, F. Kūlahcı, Z. Şen, Spatiotemporal Modeling and Simulation of Chernobyl Radioactive Fallout in Northern Turkey, *J Radioanalytical and Nuclear Chemistry* 303 (1) (2015) 171-186.
  - [5] F. Kūlahcı, Z. Şen, S. Kazanç, Cesium Concentration Spatial Distribution Modeling by PCSV, *WAS Pollution* 195 (2008) 151-160.
  - [6] I. H. Harms, Modelling the dispersion of  $^{137}\text{Cs}$  and  $^{239}\text{Pu}$  released from dumped waste in the Kara Sea. *Journal of Marine Systems* 13 (1997) 1–19.
  - [7] M. Van der Perk, T. Lev, A.G. Gillett, et al., Spatial modelling of transfer of long-lived radionuclides from soil to agricultural products in the Chernigov region, Ukraine. *Ecological Modelling* 128 (2000) 35–50.
  - [8] X. Zhang, Y. Long, X. He, J. Fu, Y. Zhang, A simplified  $^{137}\text{Cs}$  transport model for estimating erosion rates in undisturbed soil. *J Environ Radioact* 99 (2008) 1242–1246.
  - [9] J.C. Davis, *Statistics and Data Analysis in Geology*, New York, (2002) 638.
  - [10] G. Matheron, *Random Structures and Mathematical Geology*, *Revue De L Institut International De Statistique-Review of The International Statistical Institute* 38 (1) (1970).
  - [11] I. Clark, *Practical geostatistics*. Applied Science Publishers, London, 1979.
  - [12] I. Clark *Practical geostatistics*, Applied Science Publishers, London, 2001.
  - [13] F. Kūlahcı, Z. Şen, Potential utilization of the absolute point cumulative semivariogram technique for the evaluation of distribution coefficient. *J Hazard Mater* 168 (2009) 1387–1396.
  - [14] Z. Şen, Cumulative semivariogram model of regionalized variables. *Math Geol* 21 (1989) 891–903.
  - [15] Z. Şen, Z.Z. Habib, Point cumulative semivariogram of areal precipitation in mountainous regions. *J Hydrol* 205 (1998) 81–91.
  - [16] A.D. Şahin, Z. Şen, A new spatial prediction model and its application to wind records. *Theoret Appl Climatol* 79 (2004) 45–54.
  - [17] A.G. Journel, C.J. Huijbregts, *Mining geostatistics*. Academic Press, New York, 1978.
  - [18] Z. Şen, Point Cumulative Semivariogram for Identification of Heterogeneities in Regional Seismicity of Turkey. *Mathematical Geology* 30 (1998) 767-787.
- J. C. Davis, *Statistics and Data Analysis in Geology*, John Wiley & Sons Inc. Canada, 1973.